The Hidden Cost of Poor Annotations: How Label Quality Affects Camouflaged Object Detection Performance

Heny O. Velesaca[1,2], Andrea Mero[1,5], Anjali Singh[3], and Angel Sappa[1,4]

[1] ESPOL Polytechnic University, ESPOL, Campus Gustavo Galindo, Km. 30.5 Vía Perimetral, 090902, Guayaquil, Ecuador
{hvelesac,anmero,asappa}@espol.edu.ec
[2] Software Engineering Department, Research Center for Information and Communication Technologies (CITIC), University of Granada, 18071, Granada, Spain
hvelesaca@correo.ugr.es
[3] Birsa Institute of Technology, Sindri, Jharkhand University of Technology, JUT, 834010, Jharkhand, India
director@bitsindri.ac.in
[4] Computer Vision Center, Universitat Autónoma de Barcelona, 08193-Bellaterra, Barcelona, Spain
asappa@cvc.uab.es
[5] Università della Svizzera italiana(USI), Via Giuseppe Buffi 13, Lugano, Switzerland
andrea.mero@usi.ch

Abstract. This paper presents an in-depth study on the impact of high-quality, comprehensive annotations on camouflaged object detection (COD) performance. We evaluate 13 state-of-the-art COD models trained on original annotations versus a re-annotated version created under stricter, more consistent guidelines using the Cotton Bollworm dataset. Experimental results demonstrate that enhanced annotation quality significantly improves both Intersection over Union (IoU) scores and instance recall, reducing undetected camouflaged objects by an average of 4.6% in Structure-measure and 7.0% in weighted F-measure. The re-annotation process identified 1.4% additional instances, with an average area refinement of 6.3%, primarily through improvements in boundary precision and the detection of previously missed instances. These findings underscore the crucial role of precise annotations in advancing COD performance and validate the data-centric AI paradigm, suggesting that systematic refinement of annotations should be prioritized in computer vision pipelines. The re-annotated dataset is available on GitHub https://cod-espol.github.io/ReannotatedCottonBollworm/.

Keywords: Camouflaged object detection · Data-centric · Annotation quality · Pest detection · Computer vision · Dataset re-annotation.

1 Introduction

Artificial intelligence (AI) systems rely on both models and data. Most of the recent advances have concentrated on improving model architectures, where data

is often treated as *ground truth* without thorough examination of annotation quality. Recently, a new paradigm—known as data-centric AI—has emerged, first introduced by [5]. This approach emphasizes improving annotation quality rather than focusing solely on model refinement. The principle applies to all supervised learning-based methods that require annotated data for training. For instance, in the case of object detection, annotation quality is particularly crucial, as it involves not only assigning the correct class to each object but also accurately localizing all instances in an image with precise and consistent bounding boxes (e.g., [19], [6]). Similarly, in edge detection, studies have shown that precise and consistent image annotations are critical to model performance, with re-annotation efforts significantly pushing the boundaries of achievable accuracy [24]. The previous examples are just a couple of cases that benefit from the improvement in the annotations.

Data-centric AI has recently been explored in the object detection problem. In this case, studies have proven that incomplete annotations, such as when some objects of a category are left without bounding boxes, not only reduce the accuracy measured by Intersection over Union (IoU) but also introduce false negatives that can bias the learning process and degrade the model's ability to detect all instances in real-world scenarios. Therefore, the impact of high-quality annotation extends beyond a quantitative improvement in IoU; it directly affects the completeness and exhaustiveness of object detection.

In the current work, we investigate how improving annotation quality affects both the IoU-based accuracy and the model's capacity to detect every instance of interest in the camouflage object detection (COD) task. Specifically, we compare the performance of 13 SOTA COD models trained and evaluated on the original dataset annotations against that obtained using a re-annotated version created under stricter, more meticulous guidelines. Our results show that high-quality, comprehensive annotations not only boost standard performance metrics (e.g., IoU) but also improve instance recall, reducing the number of missed camouflaged objects.

The remainder of the paper is organized as follows. Section 2 summarizes works related to data-centric approaches as well as state-of-the-art camouflaged detection approaches. Section 3 describes the dataset and re-annotation process together with a short introduction of the COD approaches evaluated in the current work; additionally, the metrics used for the evaluation are introduced. Finally, Section 4 presents experimental results and discussions. Conclusions are provided in Section 5.

2 Background

Data-centric AI is based on the key understanding that data is the most important resource for creating effective and high-performing AI systems. Unlike model-centric AI development, which typically emphasizes model enhancements, data-centric AI directs attention toward methodically improving the data pipeline [34]. While data-centric AI and dataset improvement are related, they

are not equivalent. The main difference between them is that data-centric AI modifies datasets primarily to increase model accuracy, whereas dataset improvement may involve broader motivations, such as redefining a problem [20]. In the current section, some of the most relevant data-centric approaches for the object detection task are presented.

One of the seminal data-centric approaches has been presented in [20], where the authors follow specific guidelines to improve annotation quality in ImageNet and MS COCO datasets. Similarly, [2] proposes a high-quality annotation process that includes data annotations and multistage hashing to avoid duplicate instances and noisy labels. In [15], the authors highlight the importance of high-quality annotations and emphasize how inconsistent data labeling can degrade model accuracy. Maintaining annotation consistency is challenging yet essential to mitigate bias and ensure fairness in models. Additionally, the high cost of human annotation further complicates this issue. These challenges may soon drive the adoption of systematic processes to enhance data quality, particularly in annotation practices.

Object detection represents a fundamental challenge in computer vision (CV), with three primary subfields: Generic Object Detection (GOD), Salient Object Detection (SOD), and Camouflaged Object Detection (COD) [10]. A study by [6] indicates that effective data annotation practices are fundamental to object detection performance, particularly for accurate feature extraction. The current work is focused on the COD category, which specifically addresses the segmentation of visually concealed objects, typically formulated as a binary segmentation problem [18]. Recent advances in COD, as demonstrated by [36], have been facilitated by improved availability of detailed segmentation labels. However, the annotation process for camouflaged objects remains exceptionally labor-intensive, creating a critical bottleneck for research progress. This challenge aligns with [32]'s observation that supervised learning approaches are fundamentally constrained by their dependence on large-scale, high-quality datasets, a requirement particularly difficult to satisfy in real-world applications where annotation complexity and data scarcity pose substantial limitations. Building upon these foundational challenges, Section 3 systematically examines SOTA COD techniques, analyzing their performance characteristics while considering these data constraints. To our knowledge, there is no in-depth study on the relation between the results of COD approaches and the quality of camouflaged object annotations.

3 Materials & Methods

This section presents the methodology employed to evaluate the impact of annotation quality on COD performance. It describes the Cotton Bollworm dataset and re-annotation process, introduces the 13 SOTA COD techniques evaluated, and details the comprehensive evaluation metrics used for performance assessment.

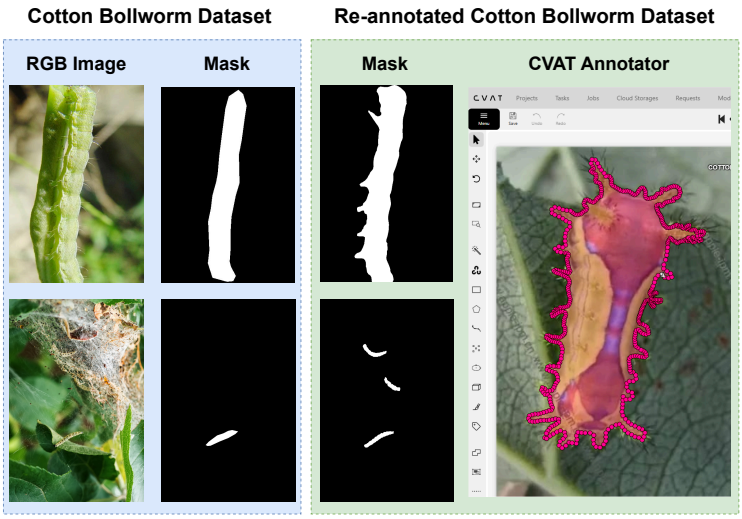

Fig. 1. Example from the Cotton Bollworm dataset: comparison between original labels *(left)* and re-annotated labels using CVAT *(right)* for camouflaged cotton bollworm detection—note how borders are better defined in the top mask, while two new instances are annotated in the bottom mask.

3.1 Dataset

In this study, the Cotton Bollworm dataset has been used. It is introduced by [22] and contains 1,073 images with an 80/15/5 split for training (856 images), validation (161 images), and testing (56 images). For re-annotation, the CVAT web-based tool[6], a specialized platform for computer vision tasks, is employed. The re-annotation process is meticulously performed for each image, adhering to the following guidelines: First, annotators were instructed to *(a)* exclusively mark worm instances while ignoring other elements, and *(b)* ensure complete coverage by annotating every visible worm without omission. Second, quality specifications required *(a)* individual polygon annotations for each worm in multi-instance images, and *(b)* pixel-precise boundary refinement to accurately capture morphological features.

Figure 1 shows examples illustrating the re-annotation pipeline that produces significant qualitative improvements. Comparing the original annotations *(left)* with the re-annotations *(right)* reveals improved morphological accuracy and the identification of previously missed worm instances.

3.2 SOTA COD Techniques

This section presents state-of-the-art (SOTA) COD techniques. Recent advances in COD have introduced diverse strategies to address the challenges of low-

[6] `https://www.cvat.ai`

Table 1. Distinctive characteristics of the evaluated SOTA COD techniques.

Technique	Source	Source Type	Year	Image Size (px)	Backbone	#Param. (M)
BASNet [25]	CVPR	Conference	2019	256×256	ResNet-34 [12]	87.06
SINet-v2 [9]	TPAMI22	Journal	2021	352×352	Res2Net-50 [11]	24.93
BGNet [4]	IJCAI22	Conference	2022	416×416	Res2Net-50 [11]	77.80
C^2F-Net [3]	TCSVT22	Conference	2022	352×352	Res2Net-50 [11]	26.36
OCENet [17]	WACV	Conference	2022	352×352	ResNet-50 [12]	58.17
EAMNet [26]	ICME	Conference	2023	384×384	Res2Net-50 [11]	30.51
DGNet [14]	MIR	Journal	2023	352×352	EfficientNet [28]	8.30
HitNet [13]	AAAI-23	Conference	2023	352×352	PVTv2 [31]	25.73
PCNet [33]	arXiv	-	2024	352×352	PVTv2 [31]	27.66
ARNet [29]	ICMR25	Conference	2025	416×416	SMT-Tiny [16]	12.82
CHNet [30]	ICMR25	Conference	2025	416×416	SMT-Tiny [16]	11.20
CTF-Net [35]	CVIU	Journal	2025	384×384	PVTv2 [31]	64.48
DRRNet [27]	arXiv	-	2025	384×384	PVTv2 [31]	89.11

contrast boundaries and complex backgrounds. BASNet [25] employs a predict-and-refine approach with a hybrid loss (BCE, SSIM, IoU), where SSIM implicitly enhances edges but lacks explicit edge modeling. SINet [9] adopts a biologically inspired search-and-identification pipeline, explicitly leveraging edge cues to locate and segment camouflaged objects. EAMNet [26] introduces dual parallel branches for segmentation and edge detection, with cross-refinement explicitly integrating edge information into the learning process. CHNet [30] focuses on channel reconstruction and hybrid attention for multi-scale feature consistency but omits explicit edge supervision. HitNet [13] iteratively refines predictions using feedback loops, indirectly improving boundary clarity without dedicated edge modeling.

For global-local feature integration, CTF-Net [35] combines CNN-based local features with Transformer-based global context, enhancing boundary precision implicitly. ARNet [29] refines features through channel interaction, implicitly improving boundaries. In contrast, BGNet [4] introduces an explicit boundary-guidance branch to model object contours directly. C^2F-Net [3] leverages cross-level context fusion, implicitly reinforcing edges for structural coherence. DGNet [14] explicitly captures edges via gradient flow to detect subtle contrast changes in low-texture regions. DRRNet [27] employs macro-micro fusion and dual reverse refinement, sharpening boundaries through explicit edge cues.

For domain-specific challenges, PCNet [33] targets plant camouflage with multi-scale refinement, explicitly addressing irregular plant edges. Finally, OCENet [17] models aleatoric uncertainty to dynamically supervise high-uncertainty regions (e.g., boundaries), implicitly improving edge detection. These methods collectively advance COD by balancing explicit edge guidance with implicit boundary refinement, tailored to diverse camouflage scenarios. Table 1 shows distinctive characteristics of the evaluated SOTA COD techniques.

3.3 Evaluation Metrics

This study employs five widely recognized evaluation metrics to assess COD performance. These metrics provide comprehensive assessment criteria for analyzing detection accuracy and effectiveness across different models: the Structure-measure (S_α) [7], weighted F-measure (F_β^w) [21], Mean Absolute Error (M) [23], E-measure (E_ϕ) [8], and F-measure (F_β) [1].

The S_α metric quantifies structural similarity between predicted and ground truth maps, measuring how well the overall structural information is preserved. The F_β^w represents an enhanced evaluation metric that extends the traditional F_β by incorporating spatial weights, delivering improved assessment of segmentation quality with emphasis on boundary precision and spatial importance of detected pixels. The M metric evaluates pixel-level errors between normalized predictions and ground truth, providing a direct measurement of prediction accuracy. The E_ϕ metric simultaneously assesses both global and local detection accuracy based on human visual perception mechanisms, offering a perceptually grounded evaluation approach. Finally, the F_β provides a balanced metric that integrates both precision and recall components to evaluate overall detection performance.

For both F-measure and E-measure metrics, different scores are computed according to various precision-recall pairs. This leads to the calculation of F-measure adaptive (F_β^{adp}), mean F-measure (F_β^{mean}), and maximum F-measure (F_β^{max}). Similarly, the E-measure employs maximum and mean variants, denoted as E_ϕ^{adp}, E_ϕ^{mean}, and E_ϕ^{max}, which are also utilized as evaluation metrics.

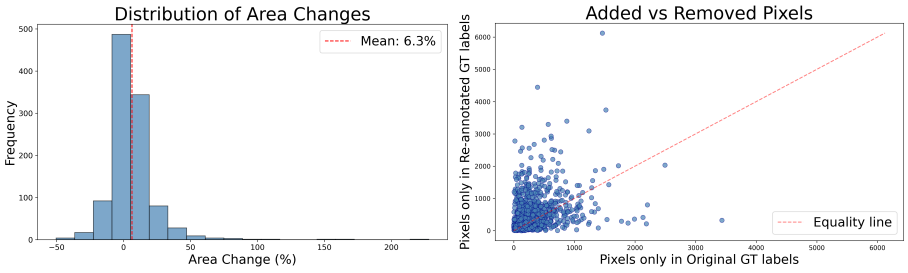

Fig. 2. *(left)* Histogram shows the distribution of percentage area changes between the original and re-annotated labels. *(right)* Scatter plot shows the number of pixels added and removed per image. dots near the red line indicate no pixel variation.

4 Results and Discussion

The experimental results demonstrate significant improvements across all evaluated SOTA COD techniques when trained on the re-annotated labels compared to the original dataset.

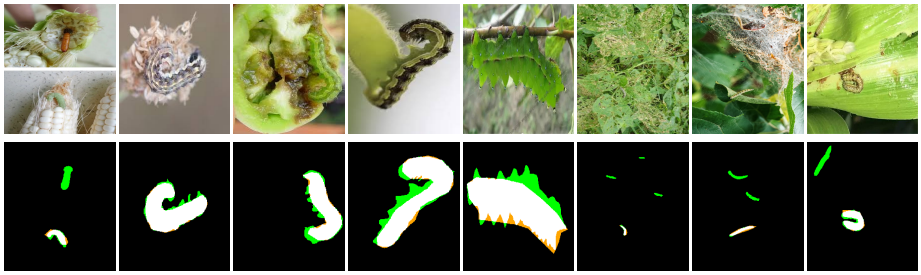

Fig. 3. Comparison between the original and re-annotated GT labels. The white areas represent matches between the original and re-annotated GT labels; the orange areas show removed pixels in the re-annotated GT labels; and the green areas show added pixels in the re-annotated GT labels.

Table 2. Evaluation metrics for each SOTA COD technique according to the metrics described in Section 3.3 using original and re-annotated datasets. The top three results are highlighted in red (first), blue (second), and green (third) respectively.

	Technique	$S_\alpha \uparrow$	$F_\beta^w \uparrow$	$M \downarrow$	$E_\phi^{adp} \uparrow$	$E_\phi^{mean} \uparrow$	$E_\phi^{max} \uparrow$	$F_\beta^{adp} \uparrow$	$F_\beta^{mean} \uparrow$	$F_\beta^{max} \uparrow$
Original Dataset	BASNet [25]	0.7860	0.6839	0.0277	0.8938	0.8811	0.8890	0.7085	0.7073	0.7235
	SINet-v2 [9]	0.8588	0.7979	0.0184	0.9430	0.9571	0.9727	0.7837	0.8086	0.8392
	BGNet [4]	0.8573	0.7964	0.0185	0.9588	0.9532	0.9625	0.8264	0.8323	0.8527
	C^2F-Net [3]	0.8399	0.7184	0.0214	0.9368	0.9329	0.9441	0.7910	0.7989	0.8215
	OCENet [17]	0.8598	0.8042	0.0164	0.9421	0.9543	0.9647	0.7809	0.8115	0.8416
	EAMNet [26]	0.8627	0.8136	0.0174	0.9576	0.9611	0.9686	0.8164	0.8320	0.8570
	DGNet [14]	0.8565	0.8005	0.0163	0.9468	0.9585	0.9666	0.7827	0.8096	0.8377
	HitNet [13]	0.8422	0.7978	0.0178	0.9601	0.9663	0.9724	0.7991	0.8060	0.8244
	PCNet [33]	0.8463	0.7885	0.0184	0.9342	0.9471	0.9642	0.7691	0.7924	0.8311
	ARNet [29]	0.8842	0.8359	0.0144	0.9556	0.9691	0.9809	0.8150	0.8501	0.8738
	CHNet [30]	0.8738	0.8276	0.0153	0.9658	0.9695	0.9757	0.8156	0.8340	0.8601
	CTF-Net [35]	0.8636	0.8195	0.0170	0.9547	0.9610	0.9697	0.8117	0.8265	0.8519
	DRRNet [27]	0.8171	0.7401	0.0218	0.9320	0.9337	0.9411	0.7462	0.7536	0.7693
Re-annotated Dataset	BASNet [25]	0.8335	0.7500	0.0242	0.9270	0.9049	0.9194	0.7538	0.7702	0.7866
	SINet-v2 [9]	0.9010	0.8677	0.0136	0.9668	0.9662	0.9723	0.8483	0.8685	0.8909
	BGNet [4]	0.8953	0.8769	0.0133	0.9708	0.9635	0.9819	0.8757	0.8864	0.9055
	C^2F-Net [3]	0.8861	0.7758	0.0178	0.9483	0.9341	0.9489	0.8369	0.8571	0.8879
	OCENet [17]	0.9071	0.8692	0.0108	0.9586	0.9622	0.9732	0.8431	0.8674	0.8964
	EAMNet [26]	0.8968	0.8610	0.0130	0.9665	0.9675	0.9757	0.8635	0.8844	0.9155
	DGNet [14]	0.9001	0.8725	0.0104	0.9615	0.9590	0.9632	0.8525	0.8747	0.8954
	HitNet [13]	0.8945	0.8633	0.0126	0.9674	0.9640	0.9673	0.8657	0.8685	0.8825
	PCNet [33]	0.9000	0.8652	0.0125	0.9651	0.9647	0.9695	0.8532	0.8657	0.8902
	ARNet [29]	0.9065	0.8814	0.0117	0.9811	0.9617	0.9779	0.8835	0.8988	0.9142
	CHNet [30]	0.9274	0.9140	0.0088	0.9812	0.9810	0.9867	0.8949	0.9157	0.9352
	CTF-Net [35]	0.9235	0.9133	0.0089	0.9829	0.9802	0.9874	0.8977	0.9134	0.9356
	DRRNet [27]	0.8794	0.8563	0.0137	0.9599	0.9572	0.9599	0.8606	0.8575	0.8606

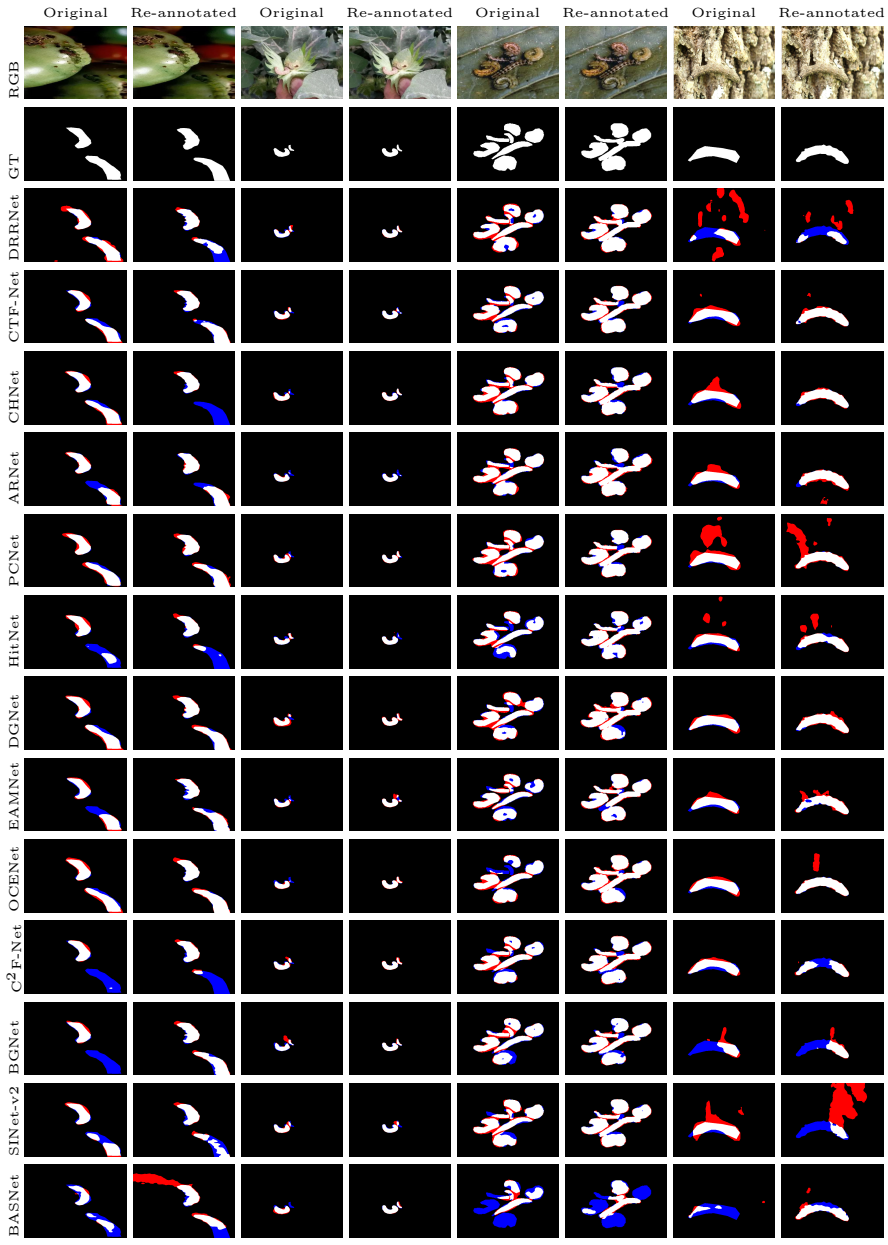

Fig. 4. Prediction results of 13 SOTA COD techniques trained with original and re-annotated labels. White areas represent successful matches between GT and predicted masks; red areas denote false positive regions (over-segmentation); and blue areas indicate false negative regions (miss-segmentation).

Table 3. Percentage difference between the results obtained for each SOTA COD technique using the original and re-annotated dataset shown in Table 2. Positive values indicate improvement in models using re-annotated labels, while negative values indicate deterioration in performance. The last row shows the improvement (%) results of the training models using the re-annotated dataset compared to the original dataset.

Technique	ΔS_α	ΔF_β^w	ΔM	ΔE_ϕ^{adp}	ΔE_ϕ^{mean}	ΔE_ϕ^{max}	ΔF_β^{adp}	ΔF_β^{mean}	ΔF_β^{max}
BASNet [25]	+4.8%	+6.6%	-0.4%	+3.3%	+2.4%	+3.0%	+4.5%	+6.3%	+6.3%
SINet-v2 [9]	+4.2%	+7.0%	-0.5%	+2.4%	+0.9%	+0.0%	+6.5%	+6.0%	+5.2%
BGNet [4]	+3.8%	+8.1%	-0.5%	+1.2%	+1.0%	+1.9%	+4.9%	+5.4%	+5.3%
C^2F-Net [3]	+4.6%	+5.7%	-0.4%	+1.2%	+0.1%	+0.5%	+4.6%	+5.8%	+6.6%
OCENet [17]	+4.7%	+6.5%	-0.6%	+1.7%	+0.8%	+0.8%	+6.2%	+5.6%	+4.5%
EAMNet [26]	+3.4%	+4.7%	-0.4%	+0.9%	+0.6%	+0.7%	+4.7%	+5.2%	+5.9%
DGNet [14]	+4.4%	+7.2%	-0.6%	+1.5%	+0.0%	-0.3%	+7.0%	+6.5%	+5.8%
HitNet [13]	+5.2%	+6.6%	-0.5%	+0.7%	-0.2%	-0.5%	+6.7%	+6.3%	+5.8%
PCNet [33]	+5.4%	+7.7%	-0.6%	+3.1%	+1.8%	+0.5%	+8.4%	+7.3%	+5.9%
ARNet [29]	+2.2%	+4.6%	-0.3%	+2.6%	-0.7%	-0.3%	+6.9%	+4.9%	+4.0%
CHNet [30]	+5.4%	+8.6%	-0.7%	+1.5%	+1.2%	+1.1%	+7.9%	+8.2%	+7.5%
CTF-Net [35]	+6.0%	+9.4%	-0.8%	+2.8%	+1.9%	+1.8%	+8.6%	+8.7%	+8.4%
DRRNet [27]	+6.2%	+11.6%	-0.8%	+2.8%	+2.4%	+1.9%	+11.4%	+10.4%	+9.1%
Improv.(%)	+4.6%	+7.0%	-0.5%	+1.5%	+0.9%	+0.7%	+6.7%	+6.3%	+5.9%

The total number of instances in the original dataset is 1,172 compared to 1,189 instances in the re-annotated dataset (1.4% increase), with an average area change of 6.3% and 84.5% overlap between annotations, showing the quantitative differences between the original and re-annotated datasets. Figure 2 *(left)* shows a histogram with the percentage distribution of change of areas between original and re-annotated labels. In addition, Figure 2 *(right)* shows a scatter plot where the number of pixels, per image, added and removed is shown. On the other hand, Figure 3 visualizes the annotation differences, showing that improvements primarily involve boundary refinement and detection of previously missed instances rather than wholesale changes to existing annotations. This indicates that improvements stem from both additional instance detection and refined boundary precision.

Figure 4 provides clear visual evidence of the improvements achieved through the re-annotation process. It offers a qualitative validation, showing that the 13 models trained with the re-annotated dataset deliver superior results. The comparison images demonstrate that models trained with re-annotated labels achieve more accurate segmentations, characterized by sharper boundaries and fewer false negatives (smaller blue areas). Notably, the improvement is particularly evident in the detection of small, highly camouflaged instances that are consistently missed by models trained with the original annotations.

On the other hand, to validate the qualitative results, Table 2 presents comprehensive performance metrics for all 13 evaluated models on both original and re-annotated datasets. The re-annotated labels consistently enhance model

performance across all metrics. The average improvements observed are: S_α increased by 4.6%, F_β^w by 7.0%, M decreased by 0.5%, E_ϕ^{adp} improved by 1.5%, and F_β^{adp} enhanced by 6.7%. CHNet and CTF-Net demonstrate the highest performance on the improved dataset, achieving S_α scores of 0.9274 and 0.9235, respectively, with corresponding F_β^w scores of 0.9140 and 0.9133. These recent architectures effectively leverage the enhanced annotation quality. DRRNet shows the most substantial relative improvement with 11.6% increase in F_β^w and 6.2% in S_α on improved annotations. This suggests that newer architectures may be more sensitive to annotation quality improvements. All models demonstrate consistent improvements across multiple metrics, with particularly notable gains in boundary-related measures (F_β^w) and structural similarity (S_α), indicating that improved annotations primarily benefit precise localization and edge detection.

Also, to measure the difference in improvement using each model and the re-annotated one vs. the original dataset, the percentage improvements are shown in Table 3, where it is demonstrated that all models benefit from re-annotating labels, with improvements ranging from 2.2% to 6.2% for S_α and 4.6% to 11.6% for F_β^w. The consistency of these improvements across diverse architectures confirms the importance of annotation quality in COD tasks.

5 Conclusion

This study provides compelling evidence for the critical importance of high-quality annotations in COD. Through comprehensive evaluation of 13 SOTA COD models on both original and re-annotated labels of the Cotton Bollworm dataset [22], we demonstrate that enhanced annotation quality consistently improves performance across all evaluated metrics and architectures. The key findings include: 1) performance improvements across all 13 evaluated models, with average gains of 4.6% in S_α and 7.0% in F_β^w; 2) Particularly significant improvements in boundary-related metrics, indicating that annotation quality primarily affects precise localization capabilities; 3) Validation of the data-centric AI approach, showing that systematic annotation improvement can be more effective than architectural modifications alone. The improved annotations resulted in 1.4% more detected instances and a 6.3% average area refinement. This demonstrates that the improvements stem from both additional instance detection and enhanced boundary precision, rather than fundamental changes to the existing annotations. These findings have important implications. First, this suggests that many existing datasets may have annotation quality limitations that artificially constrain model performance. Second, this validates the importance of investing in systematic annotation improvement processes. Finally, this demonstrates that the data-centric AI paradigm can provide substantial performance gains in challenging computer vision tasks like COD.

Acknowledgments. This work is supported by the Air Force Office of Scientific Research Under Award FA9550-24-1-0206; in part by the ESPOL project "Advancing Camouflaged Object Detection with a cost-effective Cross-Spectral vision system (ACODCS)" (CIDIS-003-2024).

References

1. Achanta, R., Hemami, S., Estrada, F., Susstrunk, S.: Frequency-tuned salient region detection. In: Conf. on Computer Vision and Pattern Recognition. pp. 1597–1604. IEEE (2009)
2. Bhatt, N., Bhatt, N., Prajapati, P., Sorathiya, V., Alshathri, S., El-Shafai, W.: A data-centric approach to improve performance of deep learning models. Scientific Reports **14**(1), 22329 (2024)
3. Chen, G., Liu, S.J., Sun, Y.J., Ji, G.P., Wu, Y.F., Zhou, T.: Camouflaged object detection via context-aware cross-level fusion. Transactions on Circuits and Systems for Video Technology **32**(10), 6981–6993 (2022)
4. Chen, T., Xiao, J., Hu, X., Zhang, G., Wang, S.: Boundary-guided network for camouflaged object detection. Knowledge-based systems **248**, 108901 (2022)
5. DeepLearningAI: A chat with andrew on mlops: From model-centric to data-centric ai (2021), `https://www.youtube.com/watch?v=06-AZXmwHjo`
6. Dong, J., Lee, J., Fuentes, A., Xu, M., Yoon, S., Lee, M.H., Park, D.S.: Data-centric annotation analysis for plant disease detection: Strategy, consistency, and performance. Frontiers in plant science **13**, 1037655 (2022)
7. Fan, D.P., Cheng, M.M., Liu, Y., Li, T., Borji, A.: Structure-measure: A new way to evaluate foreground maps. In: Int. Conference on Computer Vision. pp. 4548–4557 (2017)
8. Fan, D.P., Gong, C., Cao, Y., Ren, B., Cheng, M.M., Borji, A.: Enhanced-alignment measure for binary foreground map evaluation. arXiv (2018)
9. Fan, D.P., Ji, G.P., Cheng, M.M., Shao, L.: Concealed object detection. Transactions on pattern analysis and machine intelligence **44**(10), 6024–6042 (2021)
10. Fan, D.P., Ji, G.P., Sun, G., Cheng, M.M., Shen, J., Shao, L.: Camouflaged object detection. In: Conf. on Computer Vision and Pattern Recognition (June 2020)
11. Gao, S.H., Cheng, M.M., Zhao, K., Zhang, X.Y., Yang, M.H., Torr, P.: Res2net: A new multi-scale backbone architecture. Transactions on pattern analysis and machine intelligence **43**(2), 652–662 (2019)
12. He, K., Zhang, X., Ren, S., Sun, J.: Deep residual learning for image recognition. In: Conf. on Computer Vision and Pattern Recognition. pp. 770–778 (2016)
13. Hu, X., Wang, S., Qin, X., Dai, H., Ren, W., Luo, D., Tai, Y., Shao, L.: High-resolution iterative feedback network for camouflaged object detection. In: Conf. on Artificial Intelligence. vol. 37, pp. 881–889 (2023)
14. Ji, G.P., Fan, D.P., Chou, Y.C., Dai, D., Liniger, A., Van Gool, L.: Deep gradient learning for efficient camouflaged object detection. Machine Intelligence Research **20**(1), 92–108 (2023)
15. Kumar, S., Datta, S., Singh, V., Singh, S.K., Sharma, R.: Opportunities and challenges in data-centric ai. IEEE Access **12**, 33173–33189 (2024)
16. Lin, W., Wu, Z., Chen, J., Huang, J., Jin, L.: Scale-aware modulation meet transformer. In: Int. Conf. on Computer Vision. pp. 6015–6026 (2023)
17. Liu, J., Zhang, J., Barnes, N.: Modeling aleatoric uncertainty for camouflaged object detection. In: Winter conference on applications of computer vision. pp. 1445–1454 (2022)
18. Lv, Y., Zhang, J., Dai, Y., Li, A., Barnes, N., Fan, D.P.: Toward deeper understanding of camouflaged object detection. Transactions on Circuits and Systems for Video Technology **33**(7), 3462–3476 (2023)
19. Ma, J., Ushiku, Y., Sagara, M.: The effect of improving annotation quality on object detection datasets: A preliminary study. In: Proceedings Of The IEEE/CVF conference on computer vision and pattern recognition. pp. 4850–4859 (2022)

20. Ma, J., Ushiku, Y., Sagara, M.: The effect of improving annotation quality on object detection datasets: A preliminary study. In: Conf. on Computer Vision and Pattern Recognition Workshops. pp. 4850–4859 (June 2022)
21. Margolin, R., Zelnik-Manor, L., Tal, A.: How to evaluate foreground maps? In: Conf. on Computer Vision and Pattern Recognition. pp. 248–255 (2014)
22. Meng, K., Xu, K., Cattani, P., Mei, S.: Camouflaged cotton bollworm instance segmentation based on pvt and mask r-cnn. Computers and Electronics in Agriculture **226**, 109450 (2024)
23. Perazzi, F., Krähenbühl, P., Pritch, Y., Hornung, A.: Saliency filters: Contrast based filtering for salient region detection. In: Conf. on Computer Vision and Pattern Recognition. pp. 733–740. IEEE (2012)
24. Poma, X.S., Riba, E., Sappa, A.: Dense extreme inception network: Towards a robust cnn model for edge detection. In: Proceedings of the IEEE/CVF winter conference on applications of computer vision. pp. 1923–1932 (2020)
25. Qin, X., Zhang, Z., Huang, C., Gao, C., Dehghan, M., Jagersand, M.: Basnet: Boundary-aware salient object detection. In: Conf. on Computer Vision and Pattern Recognition (June 2019)
26. Sun, D., Jiang, S., Qi, L.: Edge-aware mirror network for camouflaged object detection. In: Int. Conf. on Multimedia and Expo. pp. 2465–2470. IEEE (2023)
27. Sun, J., Fang, X., Guan, J., Gui, D., Wang, T., Zhu, T.: Drrnet: Macro-micro feature fusion and dual reverse refinement for camouflaged object detection. arXiv preprint arXiv:2505.09168 (2025)
28. Tan, M., Le, Q.: Efficientnet: Rethinking model scaling for convolutional neural networks. In: Int. conf. on machine learning. pp. 6105–6114. PMLR (2019)
29. Wang, K., Li, X., Bai, Y., Li, S., Lu, M., Jia, Z.: Assisted refinement network based on channel information interaction for camouflaged object detection. In: Int. Conf. on Multimedia Retrieval. pp. 2058–2062 (2025)
30. Wang, K., Li, X., Li, S., Bai, Y., Li, B., Lu, M., Jia, Z.: Efficient camouflaged object detection network based on channel reconstruction and hybrid attention. In: Int. Conf. on Multimedia Retrieval. pp. 2063–2067 (2025)
31. Wang, W., Xie, E., Li, X., Fan, D.P., Song, K., Liang, D., Lu, T., Luo, P., Shao, L.: Pvt v2: Improved baselines with pyramid vision transformer. Computational Visual Media **8**(3), 415–424 (2022)
32. Xiao, F., Hu, S., Shen, Y., Fang, C., Huang, J., He, C., Tang, L., Yang, Z., Li, X.: A survey of camouflaged object detection and beyond. arXiv (2024)
33. Yang, J., Wang, Q., Zheng, F., Chen, P., Leonardis, A., Fan, D.P.: Plantcamo: Plant camouflage detection. arXiv (2024)
34. Zha, D., Bhat, Z.P., Lai, K.H., Yang, F., Jiang, Z., Zhong, S., Hu, X.: Data-centric artificial intelligence: A survey. ACM Comput. Surv. **57**(5) (Jan 2025). https://doi.org/10.1145/3711118, https://doi.org/10.1145/3711118
35. Zhang, D., Wang, C., Wang, H., Fu, Q., Li, Z.: An effective cnn and transformer fusion network for camouflaged object detection. Computer Vision and Image Understanding p. 104431 (2025)
36. Zhang, J., Zhang, R., Shi, Y., Cao, Z., Liu, N., Khan, F.S.: Learning camouflaged object detection from noisy pseudo label. In: European Conf. on Computer Vision. pp. 158–174. Springer (2024)